JOURNAL OF SOLID STATE CHEMISTRY 7, 1–6 (1973)

Ionic Conductivity of Lead Bromide Crystals

HIDEOKI HOSHINO, SHINICHI YOKOSE, AND MITSUO SHIMOJI

Department of Chemistry, Faculty of Science, Hokkaido University, Sapporo, Japan

Received April 3, 1972

The ionic conductivity of pure and NaBr-doped $PbBr_2$ crystals has been measured in the temperature range 60–320°C and in the impurity content range up to 3×10^{-3} mole fraction. The data show that the effect of association between impurity cations and anion vacancies is too large to be neglected. The mobility, μ, the concentration, x_n^0, of anion vacancies and the association constant, K_3, are obtained, respectively, as follows:

$$\mu = (0.84/T)\exp(-0.23\,\text{eV}/kT)(\text{cm}^2/\text{V sec}),$$

$$x_n^0 = 3.2 \times 10^2 \exp(-0.60\,\text{eV}/kT)\,(\text{mole fraction})$$

and

$$K_3 = 0.12\exp(+0.25\,\text{eV}/kT)\,(\text{mole fraction})^{-1}.$$

The measurements have also been made on pressed pellets of pure and KBr-doped $PbBr_2$, whose conductivity values are higher than those of the crystals.

1. Introduction

Some physical properties of $PbBr_2$, which is known as an anionic conductor (*1*), have been investigated by various authors (*2–7*). As in the case of $PbCl_2$ (*8*), the Schottky-type disorder is supposed to be dominant in $PbBr_2$ crystals owing to the large size of the bromide ions and the narrow free space around an interstitial site (*7, 9, 10*). By assuming that the transport number of anion vacancies is unity in all the experimental temperature ranges (50–300°C), Verwey and Schoonman (*6*) have determined the energy of formation of the intrinsic lattice defects and the energy for migration from the slopes of the conductivity curves of $PbBr_2$ crystals doped with Ag^+, Cu^+, and Tl^+ ions and have estimated (*11*) the concentration and the mobility of mobile lattice defects (in the case of Tl^+ ions) as a function of temperature without considering the effects of entropy and impurity–vacancy association. These previous insufficiencies have been resolved in the recent work of Schoonman (*7*). He has determined the values of entropy for the Tl^+-doped $PbBr_2$ samples in which the association effect was not observed. He has also reported the effects of association and precipitation for the CuBr-doped $PbBr_2$ crystal. In the present paper, the Na^+ ions are employed as monovalent cation impurities, excluding the effect of *d* electrons expected for Cu^+ ions (*7*).

This paper describes the result of the ionic conductivity measurements (i) on single crystals of pure and highly NaBr-doped $PbBr_2$ and (ii) on "pellets" of pure and KBr-doped $PbBr_2$. The data for the crystals containing Na^+ ions showed an existence of associated species between Na^+ ions and anion vacancies.

2. Experimental

The $PbBr_2$ solid was precipitated by mixing aqueous solutions of lead nitrate (analytical grade) and hydrobromic acid (analytical grade). After drying in a vacuum at 100°C the $PbBr_2$ powder was melted in a sealed pyrex glass ampoule. Crystals for measurements were obtained by the Bridgman method, and the purity of the pure crystals was considered to be nearly the same as that in the measurement of Verwey and Schoonman (*6*) because of the good agreement in the conductivity data (see Fig. 1). Although Modestova (*12*) found some phase transition in $PbBr_2$ at 344°C, we had no difficulty in preparing our crystals. The crystals were

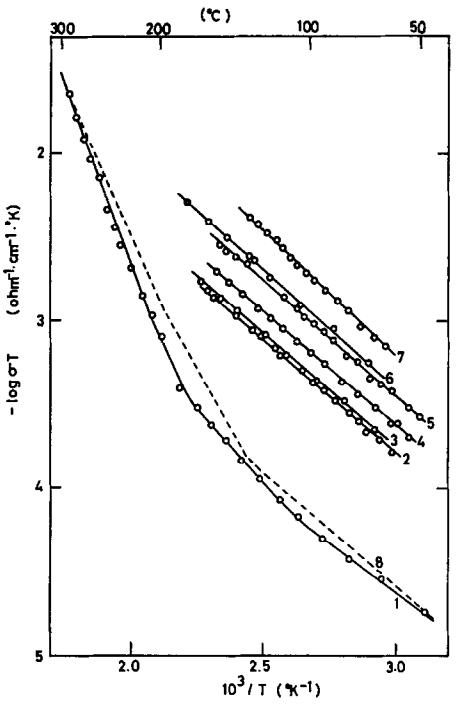

FIG. 1. Ionic conductivity, σ, of $PbBr_2$ crystals plotted as $\log \sigma T$ versus $10^3/T$. (1) pure $PbBr_2$, (2) doped with 5.2×10^{-4} NaBr, (3) doped with 5.9×10^{-4} NaBr, (4) doped with 7.5×10^{-4} NaBr, (5) doped with 1.22×10^{-3} NaBr, (6) doped with 1.5×10^{-3} NaBr, (7) doped with 3.0×10^{-3} NaBr, and (8) pure $PbBr_2$ due to Verwey and Schoonman (*6*).

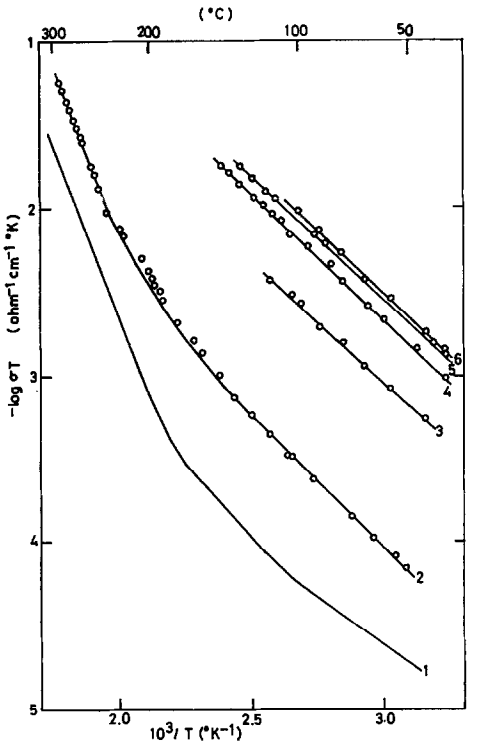

FIG. 2. Ionic conductivity, σ, of $PbBr_2$ pellets plotted as $\log \sigma T$ versus $10^3/T$. (1) pure $PbBr_2$ crystal, (2) pure $PbBr_2$ pellet, (3) doped with 5.0×10^{-4} KBr, (4) doped with 7.5×10^{-4} KBr, (5) doped with 3.0×10^{-3} KBr, and (6) doped with 5.0×10^{-3} KBr.

cleaved perpendicular to the <100> direction. Cloudiness due to precipitation of NaBr was not observed. The concentrations of NaBr were determined by means of flame photometry. The pellets, 13 mm in diameter and about 1 mm thick, were pressed from the solidified products under about 6 tons/cm^2. The density of the pellets was about 96% of the ideal value. The concentration of KBr was determined from the amounts weighed into the melts because of the low sensitivity in the flame photometry. Other experimental arrangements and techniques were the same as before (*8*). The conductivity measurements were limited to temperatures below 320°C.

3. Results

The conductivity data for the single crystals are shown in Fig. 1 and those for the pellets in Fig. 2. The experimental errors are about ±5%. Figure 1 indicates that the present conductivity values for pure single crystals are in agreement with those due to Verwey and Schoonman (*6*). The conductivity σ increases with the NaBr concentration, and that of the pellets is larger

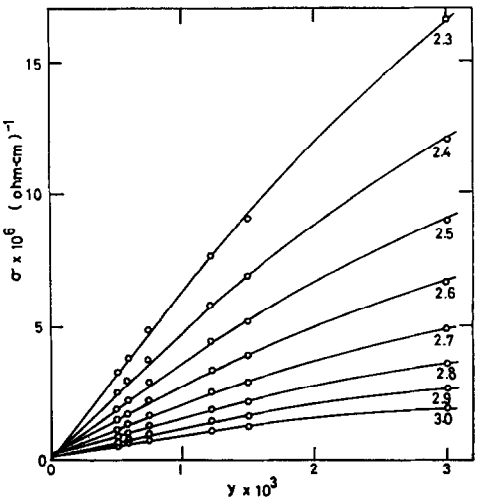

FIG. 3. σ as a function of the concentration of NaBr, y. The numbers on the isotherms are the values of $10^3/T$.

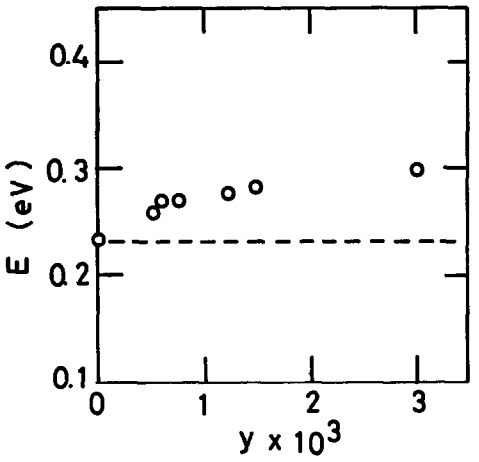

FIG. 4. Apparent activation energy, E, as a function of the concentration of NaBr, y. The dotted line displays the activation energy for migration of anion vacancy, 0.23 eV, which is obtained from the conductivity data of NaBr-doped $PbBr_2$ crystals with the aid of the analysis of Eq. (1).

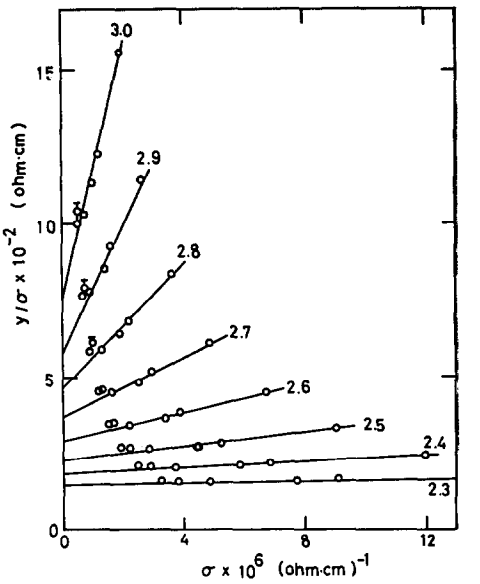

FIG. 5. y/σ as a function of σ. The numbers on the isotherms are the values of $10^3/T$.

than that of the crystals in both the pure and doped states. In Fig. 3 the conductivity values, σ, of the $PbBr_2$ crystals doped with NaBr are plotted as a function of the concentration of NaBr, y. These plots show that a linearly extrapolated line does not always pass the origin as temperature is lowered. Further, the slope of $\log\sigma T$–$1/T$ curves shown in Fig. 1 increases with increase of impurity concentration as shown in Fig. 4. These facts suggest an existence of associated species (*13*).

4. Analysis of Results

In $PbBr_2$, as reported in the previous studies (*1*, *6*, *7*) the anion vacancies are considered to be the dominant charge carriers over all the experimental temperature ranges and the addition of NaBr may produce anion vacancies (*1*, *6*); the Na^+ ions and the anion vacancies interact on each other to form a complex because of their opposite effective charges. Another association may occur between intrinsic lattice defects because of the large negative effective charge on cation vacancies, as proposed by Simkovich (*14*). Under these conditions the concentration of monovalent impurity cations, y, is related to the conductivity of a doped sample, σ, as shown in Eq. (A5) in the Appendix. In Fig. 5 the isothermal plots of y/σ versus σ for the $PbBr_2$ crystals doped with NaBr show a good linearity within experimental errors. This shows that the effect of the associates due to intrinsic vacancies is negligible in this case. In other words, Eq. (A5) can be approximated by the first two terms arranged as follows:

$$y = A\sigma^2 + B\sigma, \tag{1}$$

where

$$A = K_3(x_n^0)^2/\sigma_0^2 \text{ and } B = x_n^0/\sigma_0.$$

The definitions for K_3, x_n^0, and σ_0 are given in the Appendix. Equation (1) is the same expression as presented by Etzel and Maurer (*15*). The temperature dependence of A and B, obtained from the plots in Fig. 5, is shown in Fig. 6. The mobility, μ, can be represented experimentally by

$$\mu = \sigma_0/eNx_n^0 = M/BF\rho$$
$$= [(0.84 \pm 0.15)/T] \exp(-0.23 \pm 0.02\,\text{eV}/kT) \quad (\text{cm}^2/\text{V sec}). \tag{2}$$

In this equation, e is the protonic charge, N the number of ion pairs per unit volume of $PbBr_2$, M the molecular weight, ρ the density of the sample and F the Faraday constant. Comparing Eq. (2) with the theoretical expression (*8*, *13*), we find that the activation energy for migration, $U_m = 0.23 \pm 0.02$ eV and the factor (*13*), $\nu_0 \exp(\Delta S_m/k) = (4.8 \pm 0.7) \times 10^{10}\,\text{sec}^{-1}$ using 3.9 Å for the cation–anion separation (*11*).

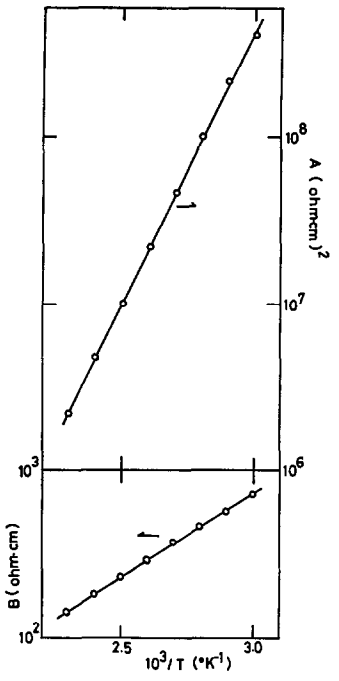

FIG. 6. Slopes A and intercepts B as a function of $10^3/T$.

The conductivity of the pure $PbBr_2$ crystals in the intrinsic region, σ_0, shown in Fig. 1, is arranged in the form of

$$\sigma_0 T = (5.0 \pm 0.8) \times 10^5 \exp(-0.83 \pm 0.04\,\mathrm{eV}/kT)(\mathrm{ohm}^{-1}\mathrm{cm}^{-1}\,\mathrm{K}). \quad (3)$$

Then, the concentration of the intrinsic anion vacancy (in mole fraction) is expressed from Eq. (1) as follows:

$$x_n^0 = \sigma_0 B = (3.2 \pm 0.4) \times 10^2 \exp(-0.60 \pm 0.04\,\mathrm{eV}/kT). \quad (4)$$

The comparison of Eq. (4) with the theoretical expression (*8*) which is obtained by assuming a complete dissociation of the intrinsic lattice defects yields that the energy of formation of a Schottky defect trio $E_s = 1.80 \pm 0.12$ eV and the corresponding entropy $\Delta S_s/k = 16 \pm 1$.

The equilibrium constant, K_3, of the reaction for the complex formation between anion vacancies and impurity cations is expressed in terms of A and B, i.e., $K_3 = A/B^2$ from Eq. (1). The temperature dependence of K_3 is given by

$$K_3 = (0.12 \pm 0.02)\exp(0.25 \pm 0.04\,\mathrm{eV}/kT)\ (\text{mole fraction})^{-1}. \quad (5)$$

From this, the energy of formation of associated pairs, E_a, becomes 0.25 ± 0.04 eV. The degree of association of impurity cations, p, is given by $(y - x_c)/y$, and can be represented as $p = 1/[(B/A\sigma) + 1]$ from Eqs. (A3), (1), and the relation $x_n/x_n^0 = \sigma/\sigma_0$. In the sample containing 1.5×10^{-3} NaBr the value of p was 0.12 at 160°C and increased to 0.41 at 60°C.

The mean values of the apparent activation energy in the extrinsic region for the pellets of pure and KBr-doped $PbBr_2$ are estimated to be 0.30 ± 0.03 eV from the plots of $\log\sigma T$ versus $1/T$ shown in Fig. 2. The apparent activation energy in the intrinsic region for the pure pellet of $PbBr_2$ is obtained as 0.82 ± 0.04 eV in the same way. These values are respectively in rough agreement with the apparent activation energy values 0.27 ± 0.07 eV and 0.83 ± 0.04 eV, which are obtained from the data for the crystals in Fig. 1 without considering any association effect represented by Eq. (1).

5. Discussion

In Table I the energy values obtained from the present measurements are compared with those of various authors. The present U_m value (0.23 eV) is in good agreement, within experimental errors, with that (0.25 eV) obtained by Schoonman (*7*) in the case of Tl^+ impurities which showed no association effects. The values obtained by Verwey and Schoonman (*6*) (0.29 eV) and by Smakula (*16*) (0.28 eV) from the plots of $\log\sigma T$ versus $1/T$ are larger than the present U_m value. This may be due to the effect of complex formation included in the plot of $\log\sigma T$ versus $1/T$.

The present E_s value (1.80 eV) is also in agreement with that of Schoonman (*7*) (1.71 eV). However, the small E_s value (1.44 eV) due to Verwey and Schoonman (*6*) may also be attributed to the neglect of complex formation.

In the present study, the Na^+ ions were employed as impurities. The ionic radius of Na^+ ions (0.95 Å) is nearly the same as that of Cu^+ ions (0.96 Å) which have been used as impurities in the Schoonman's conductivity study (*7*). However, the heat of association, E_a, between Na^+ ions and anion vacancies (0.25 eV) in the present case is slightly larger than that between Cu^+ ions and anion vacancies (0.18 eV) (*7*). This difference may be attributed to the existence of d electrons (for Cu^+ ions) or not (for Na^+ ions). Moreover, in the present analysis the equilibrium constant, K_3, of the complex formation is obtained with definite pre-exponential factor

TABLE I

CONDUCTIVITY PARAMETERS FOR $PbBr_2$ CRYSTALS

Sources	Activation energy for V_n-migration U_m (eV)	Energy of formation for three vacancies E_s (eV)	Energy of association E_a (eV)
Present measurements	0.23 ± 0.02	1.80 ± 0.12	0.25 ± 0.04 (with Na^+)
Verwey and Schoonman (*6*)	0.29 ± 0.04	1.44 ± 0.18	—
Smakula (*16*)	0.28	1.92	—
Schoonman (*7*)	0.25 ± 0.01	1.71 ± 0.09	0.18 ± 0.02 (with Cu^+)

$[0.12 \pm 0.02$ (mole fraction)$^{-1}]$, while in Schoonman's analysis (*7*) this pre-exponential value has not been given. This may also yield some difference in the E_a values.

For the expression of the mobility the pre-exponential term obtained in the present work (0.84 ± 0.15 cm^2 K/V sec) is smaller than that (10^2) obtained by Schoonman and Verwey (*11*) but close to that for $PbCl_2$ (2.6×10^{-2}) (*8*). Schoonman and Verwey (*11*) have determined the concentration of anion vacancies under the assumption that ΔS_s is zero. However, the present analysis indicates that this entropy value is (16 ± 1) k, being the same magnitude as determined for the $PbCl_2$ crystal, 16 k (*8*). It should be noted that some of his original plots of the intrinsic conductivities presented later by Schoonman (*7*) can give 12 k for the ΔS_s, being somewhat close to the present results; though in his same thesis another value 8.4 k was adopted as a compiled value.

In the simple plot of $\log \sigma T$ versus reciprocal temperature for the pure $PbBr_2$ crystals (Fig. 1) there are three different regions: the respective activation energy values are 0.23 eV for lower temperature regions, 0.83 eV for higher temperature ranges and the intermediate values for the middle temperature region. The region with 0.23 eV seems to be the extrinsic region in which the anion vacancy migration is dominant, since the activation-energy value is in good agreement with that obtained from the mobility. Moreover, Fig. 4 suggests that if an association is present between impurity ions and anion vacancies, the apparent activation energy should be larger than 0.23 eV in the extrinsic region of pure crystals. The region with 0.83 eV seems to be the intrinsic region of $PbBr_2$, in which the anion and cation vacancy are completely dissociated (*6*, *8*). The intermediate region may be a transition state from the extrinsic region to the intrinsic one; the concentration of anion vacancy, x_n, can be obtained using Eq. (A5).

Figures 1 and 2 show that the conductivity values for the crystals are smaller than those for the pellets over the whole experimental temperature range, and that the activation energies obtained on the pellets are not very different from those of the crystals. The conductivity measurement of the pellets of $PbBr_2$ has been carried out in the frequency range between 500 and 600 Hz, so that the effect due to a dielectric dispersion observed by Weaver and Lorenzoni (*17*) may be appreciable. Another transport mechanism, e.g., the diffusion along the grain boundaries (*18–22*) may be considered to interpret this difference. The details are not clear in the present work.

Appendix

In $PbBr_2$ with the Schottky-type defect, the transport number of anion is practically unity (*1*, *6*). Consider the case that the added monovalent cation impurity, I (with the concentration, y, in mole fraction), interacts on the anion vacancies, $V_n(x_n)$, to form a complex, $C(x_c)$.

Additionally, the lattice defects, V_n and $V_p(x_p)$ may produce an associate, $A(x_a)$ with the effective

charge $-e$ because of the large effective charge of cation vacancies. The following equations can then be written using respective reaction constants, K_i;

$$V_p + 2V_n = 0 \text{ and } K_1 = 1/x_n^2 x_p, \quad \text{(A1)}$$

$$V_p + V_n = A \text{ and } K_2 = x_a/x_n x_p, \quad \text{(A2)}$$

$$I + V_n = C \text{ and } K_3 = x_c/(y - x_c)x_n, \quad \text{(A3)}$$

and the electroneutrality condition is given by

$$(y - x_c) + 2x_p + x_a = x_n. \quad \text{(A4)}$$

The expression for the impurity concentrations, y, is given by solving Eqs. (A1)–(A4).

$$y = K_3(x_n^0)^2\sigma^2/\sigma_0^2 + x_n^0\sigma/\sigma_0 - K_2K_3/K_1 - \sigma_0(K_2/2^{1/3}K_1^{2/3} + 2^{2/3}K_3/K_1^{2/3})/\sigma - \sigma_0^2 x_n^0/\sigma^2, \quad \text{(A5)}$$

where x_n^0 is the concentration of the intrinsic anion vacancy, σ_0 is the conductivity value for the intrinsic region of pure crystal, and the assumption that $x_n/x_n^0 = \sigma/\sigma_0$ is adopted.

The defect model of Simkovich type (*14*) for lead halides can be expressed by using

$$A + V_n = 0 \text{ and } K_2' = 1/x_n x_a, \quad \text{(A2')}$$

and

$$(y - x_c) + x_a = x_n, \quad \text{(A4')}$$

instead of Eqs. (A2) and (A4). In this case the third term in Eq. (A5) should be read $2^{2/3}K_3K_1^{2/3}$, the fourth term $\sigma_0 x_n^0(1 + 2^{1/3}K_3/K_1^{1/3})/\sigma$ and the last term disappears. If $K_3 = 0$, this rewritten equation can be reduced to Eq. (17) in Simkovich's paper (*14*).

References

1. C. TUBANDT, *Z. Anorg. Chem.* **29**, 313 (1923).
2. J. ARENDS AND J. F. VERWEY, *Phys. Status Solidi* **23**, 137 (1967).
3. J. F. VERWEY, *J. Phys. Chem. Solids* **27**, 468 (1966); *ibid.* **31**, 163 (1970).
4. J. SCHOONMAN, *J. Solid State Chem.* **2**, 31 (1970).
5. J. F. VERWEY AND N. G. WESTERINK, *Physica* **42**, 293 (1969).
6. J. F. VERWEY AND J. SCHOONMAN, *Physica* **35**, 386 (1967).
7. J. SCHOONMAN, Thesis, University of Utrecht (1967).
8. H. HOSHINO, M. YAMAZAKI, Y. NAKAMURA, AND M. SHIMOJI, *J. Phys. Soc. Japan* **26**, 1422 (1969).
9. W. NIEUWENKAMP AND J. M. BIJVOET, *Z. Kristallogr. Kristallgeometrie Kristallphys. Kristallchem.* **84**, 49 (1933).
10. H. BRAEKKEN AND L. HARANG, *Z. Kristallogr. Kristallgeometrie Kristallphys. Kristallchem.* **68**, 123 (1928).
11. J. SCHOONMAN AND J. F. VERWEY, *Physica* **39**, 244 (1968).
12. T. MODESTOVA AND T. N. SUMAROKOVA, *Zh. Neorg. Khim.* **3**, 1655 (1958).
13. A. B. LIDIARD, "Handbuch der Physik," Vol. 20, p. 246, Springer Verlag, Berlin (1957).
14. G. SIMKOVICH, *J. Phys. Chem. Solids* **24**, 213 (1963).
15. H. W. ETZEL AND R. J. MAURER, *J. Chem. Phys.* **18**, 1003 (1953).
16. A. SMAKULA, M. I. T. Technical Report No. 6 (1965).
17. C. WEAVER AND S. LORENZONI, *Phil. Mag.* **20**, 455 (1969).
18. R. SMOLUCHOWSKI, "Imperfections in Nearly Perfect Crystals," p. 471, John Wiley and Sons, New York (1952).
19. S. AMELINCKX AND W. DEKEYSER, Solid State Phys. **8**, 327 (1959).
20. H. MYKURA, "Solid Surfaces and Interfaces," Dover Publications, New York (1966).
21. P. G. SHEWMON, "Diffusion in Solids," p. 164, McGraw-Hill (1963).
22. A. SMEKAL, "Handbuch der Physik," Vol. 24(2), p. 878, Verlag Jelius Springer, Berlin (1933).